Journal of
Biomaterials and Tissue Engineering
Vol. 4, 295–299, 2014

RESEARCH ARTICLE

Accelerated Sonochemical Synthesis of Calcium Deficient Hydroxyapatite Nanoparticles: Structural and Morphological Evolution

Namitha Varadarajan[1, †], Rajkamal Balu[2], Deepti Rana[3, ‡], Murugan Ramalingam[3, 4, 5], and T. S. Sampath kumar[2, *]

[1] *Department of Ceramic Engineering, National Institute of Technology Rourkela, Orissa 769008, India*
[2] *Medical Materials Laboratory, Department of Metallurgical and Materials Engineering, Indian Institute of Technology Madras (IITM), Chennai 600036, India*
[3] *Centre for Stem Cell Research, A unit of Institute for Stem Cell Biology and Regenerative Medicine-Bengaluru, Christian Medical College Campus, Vellore 632002, India*
[4] *Faculté de Chirurgie Dentaire, Institut National de la Santé Et de la Recherche Médicale UMR977, Université de Strasbourg, Strasbourg 67085, France*
[5] *WPI-Advanced Institute for Materials Research, Tohoku University, Sendai 980-8577, Japan*

Calcium deficient hydroxyapatite (CDHA) nanoparticles with a Ca/P ratio of 1.6 were synthesized by accelerated sonochemical process. The synthesis was carried out using calcium nitrate and diammonium hydrogen phosphate in an ultrasonic bath operated at a fixed frequency of 135 kHz and 250 Watts power. The effect of ultrasonic radiation as a function of time over the formation and structure of nanoparticles were investigated using X-ray diffraction, spectroscopy and microscopy methods. The synthesized nanocrystals showed X-ray powder diffraction pattern corresponding to that of hydroxyapatite stoichiometry with CDHA characteristics. HPO_4^{2-} Fourier transform infrared vibration band observed at 875 cm^{-1}. Transmission electron microscopic analysis confirmed the nanocrystalline nature and growth of acicular, rod and needle-like CDHA nanocrystals morphology with increasing irradiation time.

Keywords: Calcium Deficient Hydroxyapatite, Sonochemical, Nanoparticles, Structure, Morphology.

1. INTRODUCTION

Hydroxyapatite (HAp) with chemical formula $Ca_{10}(PO_4)_6(OH)_2$ and Ca/P ratio of 1.67 is a naturally occurring bioactive form of calcium phosphate with excellent biocompatibility, bioactivity and stability against bioabsorption.[1] It has a composition and crystal structure close to the human dental structure and skeletal system; therefore it is widely used in biomedical applications such as dental implants, bone substitutes, stem cell differentiation, tissue enginering, and drug delivery systems in the form of powder, porous blocks or beads.[2] Nanocrystalline HAp exhibits better bioactivity and biocompatibility with enhanced mechanical properties over microcrystalline or bulk HAp because of their unique quantum confinement effects and reactive surface area properties. Hence, these nanocrystallites can be used in designing superior biocompatible coatings for the implants and in developing high-strength nanocomposites.[3] HAp can be prepared by many routes such as sol gel,[4] homogenous precipitation,[5] hydrothermal,[6] spray dry,[7] combustion synthesis,[8] microwave irradiation,[9] ultrasonic spray freeze-drying,[10] sonochmical synthesis[11] etc. Ultrasonic irradiation in wet milling is an efficient means for grinding, dispersing, and de-agglomerating the sample particles. The acoustic cavitations forms the sonochemical effects. Acoustic cavitations i.e., the formation, growth and implosive collapse of bubbles produces intense local heating, high pressures and enormous heating and cooling rates which results into sonochemical effect in liquids help in manufacturing superfine size slurries with increased reaction speed, reaction output and more efficient energy usage. There are reports supporting nano

*Author to whom correspondence should be addressed.
†Part of summer internship work done at IITM, Chennai 600036, India.
‡Project Internship Student from Amity University, New Delhi, India.

RESEARCH ARTICLE

structured HAp powders prepared by ultrasonic-coupled sol–gel synthesis causing reduction in the particle size with ultrasonication compared to conventional sol–gel method.[12] Poinern et al. reported nanocryatalline (particle size equal to 30 nm) HAp by wet precipitation method using $Ca(NO_3)$ and KH_2PO_4 as key ingredients and NH_3 as the precipitator under ultrasonic irradiation.[13] Manafi et al. reported HAp particle shape change from spherical to rod-shape with increase in ultrasonication time in a hydrothermal route coupled with ultrasonication.[14] Hence this method can be used for nanoparticle synthesis as well as manipulating the nanoparticle's properties according to requirements.

Calcium deficient hydroxyapatite (CDHA) with chemical formula $Ca_{10-x}(HPO_4)_x(PO_4)_{6-x}(OH)_{2-x}$ is a compound formed by the loss of calcium ions from the HAp unit cell with Ca/P ratios ranging from 1.33 to 1.67, where the H_2O molecules are located on the places corresponding to the missing OH^- groups, and they are hydrogen bonded to the nearest PO_4^{3-} groups. This class of compounds presents higher resorbability and lower thermal stability than stoichiometric HAp. CDHA have various immediate biomedical applications[22,23] and can be used to mimic natural biomineralisation of bone. Above 200 °C, the HPO_4^{2-} group in CDHA transforms into $P_2O_7^{4-}$ and H_2O.[15] Rapid synthesis of nano-sized CDHA (Ca/P ratio = 1.5) particles with needle-like morphology through the reaction of $Ca_3(NO_4)_2 \cdot 4H_2O$ and H_3PO_4 by microwave irradiation has been reported[16] Although, there are several studies on the influence of ultrasonication on HAp synthesis, the influence of sonication on the CDHA formation has been not reported. By manipulating the properties of CDHA they can be used in tailor made fashion for various applications such as template for biomimetic apatite formation etc. In the present work, the effect of ultrasonic irradiation time over the structural and morphological evolution of CDHA nanoparticles is acutely investigated.

2. MATERIALS AND METHODS

All the chemicals and reagents used in this experiment were purchased from Merck, India. Nanocrystalline CDHA powder was synthesized via a simple co-precipitation method coupled with ultrasonication. Briefly, 0.8 M solution of $Ca_3(NO_4)_2 \cdot 4H_2O$ and 0.5 M solution of $(NH_4)_2HPO_4$ were prepared separately and mixed to stoichiometric Ca/P ratio of 1.6 with pH of the reaction mixture maintained at 10 throughout the reaction using ammonia solution. Formation of milky white precipitate was observed during the reaction. After complete mixing of the solution, the precipitate was subjected to ultrasonic irradiation in an ultrasonic bath (Crest Ultrasonics, USA) operated at fixed frequency of 135 kHz with power of 250 watts. The temperature of the samples was recorded periodically. The precipitate after ultrasonication was washed repeatedly with distilled water to remove unwanted ions such as NH^{4+} and NO_3^{2-}, oven dried at 100 °C and ground to a fine powder using an agate mortar and pestle.

2.1. Characterization

Samples were collected at time interval of 30 min till 150 min and characterized by X-ray powder diffraction (XRD), Fourier transform infrared (FTIR) spectroscopy, transmission electron microscopy (TEM), and selected area electron diffraction (SAED) methods. A fraction of the synthesized powder was heat treated at 650, 700 and 750 °C for 2 h in a muffle furnace to study the thermal stability and phase change.

XRD analysis was performed on D8 Discover XRD system (Bruker, USA) with Cu Kα radiation ($\lambda = 1.54$ Å) at scanning rate of 0.1°/step and 2θ ranging from 20° to 60°. The functional groups of CDHA were analyzed using Spectrum one FTIR spectrometer (Perkin-Elmer, USA). Spectra were collected in the spectral range of 4000–400 cm^{-1} using KBr pellet technique with spectral resolution of 4 cm^{-1}. The crystalline size and morphology of synthesized particles were examined with a CM20 TEM (Philips, Netherlands) supported with SAED. TEM

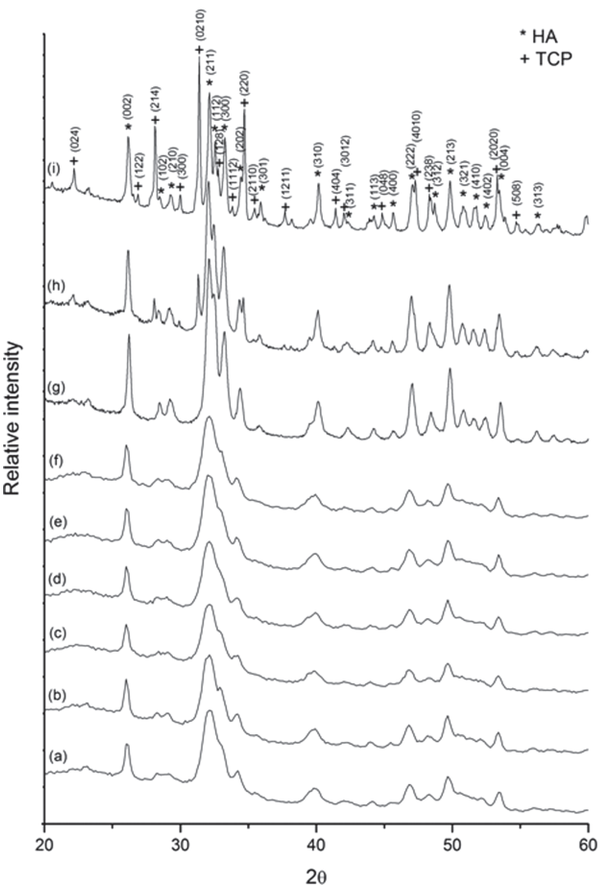

Fig. 1. XRD pattern of CDHA; (a) 0 min (b) 30 min (c) 60 min (d) 90 min (e) 120 min, and (f) 150 min sonicated samples. XRD pattern of 120 min sample heat-treated at (g) 650 °C (h) 700 °C, and (i) 750 °C.

Table I. List of cell parameters, crystallinity and crystallite size for various sonication times.

Sonication time (min)	Crystallite size (nm)	a (Å)	c (Å)	Cell volume (m^3)	Percentage crystallinity
0	24	9.426	6.844	526.71	22
30	28	9.405	6.853	525.12	25
60	28	9.404	6.850	524.68	16
90	26	9.389	6.861	523.94	21
120	24	9.399	6.838	523.03	28
150	26	9.403	6.854	524.90	31

specimens were prepared by depositing a few drops of CDHA dispersed in acetone on carbon coated copper grid and air-dried.

3. RESULTS AND DISCUSSION

The XRD pattern of the samples is shown in Figure 1. It was observed that all the samples show XRD peaks (002), (211), (112), (300), (310) similar to that of HAp (JCPDS 9-432) confirming the formed phase as apatite and absence of peaks like (024), (0210) etc. related to other phases such as β-tricalcium phosphate. The diffraction peak at 25.9° (2θ) corresponding to the (002) Miller plane family was chosen for calculation of the crystalline size, as it is isolated from other peaks and is relatively sharper than the other peaks. The average crystallite size was calculated using Scherrer's formula:[15]

$$t = K\lambda/B\ \mathrm{Cos}\theta \qquad (1)$$

Where, 't' is the average crystallite size (nm), 'K' is the shape factor ($K = 0.9$), 'λ' is the wavelength of the X-rays ($\lambda = 1.54056$ Å for Cu Kα radiation), 'B' is the full width at half maximum (radian) and 'θ' is the Bragg's diffraction angle. The cell volume and cell parameters of CDHA were calculated using Unit cell software by least-square fit method and listed in Table I.

Figure 2 shows the variation of crystallite size and sonication bath temperature with ultrasonication time. During precipitation it has been reported that the crystallite size

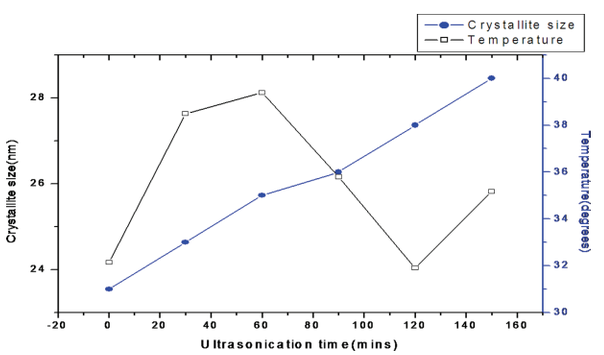

Fig. 2. Variation of crystallite size and sonication bath temperature with ultrasonication time.

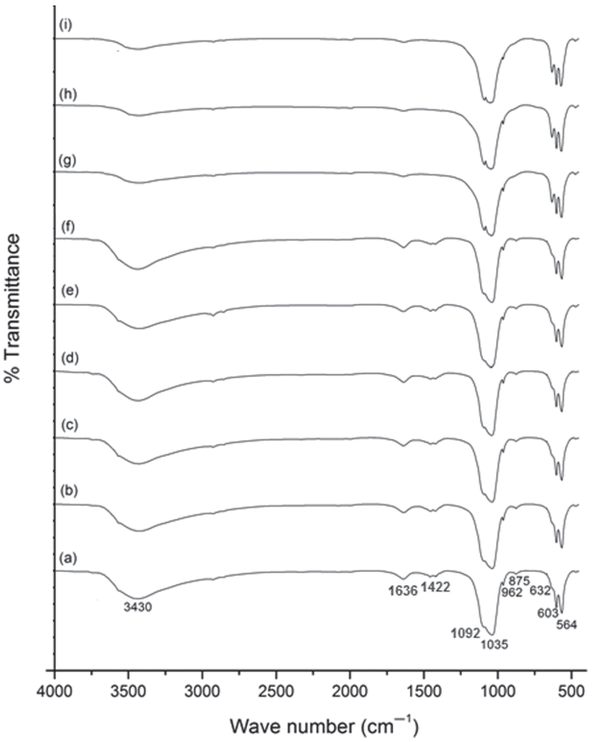

Fig. 3. FT-IR spectra of (a) Control (b) 30 min ultrasonication (c) 60 min ultrasonication (d) 90 min ultrasonication (e) 120 min ultrasonication (f) 150 min ultrasonication sample (g) 650 °C heated (h) 700 °C heated (i) 750 °C heated sample of 120 min ultrasonication sample.

increases with an increase in the reaction temperature.[17,18] But when precipitation is coupled with ultrasonication, it has been seen that the crystallite size increases for the first 60 minutes of ultrasonication and then it shows a decreasing trend for the next 60 minutes (60 to 120 min) following which the crystallite size again starts increasing. The initial rise in the crystallite size is due to the rise in the reaction temperature as in the simple precipitation process. The effect of ultrasonication is seen after 60 minutes, as a result of which there is a decrease in the

Table II. Assignments of infrared frequencies (cm^{-1}) of as synthesized and heated samples.

	Infrared frequencies (cm^{-1})	
Assignments	As synthesized (120 min sonicated)	Heat treated (700 °C)
PO_4^{3-} bend ν_2	564	566
PO_4^{3-} bend ν_4	603	601
Structural OH^{3-}	632	631
HPO_3^{2-}	875	–
PO_4^{3-} stretch ν_3	962	961
PO_4^{3-} bend ν_3	1035	1042
HPO_3^{2-}	1092	1090
$CO_3^{2-}\nu_3$	1422	–
H_2O adsorbed ν_2	1636	1632
H_2O adsorbed	3432	3434

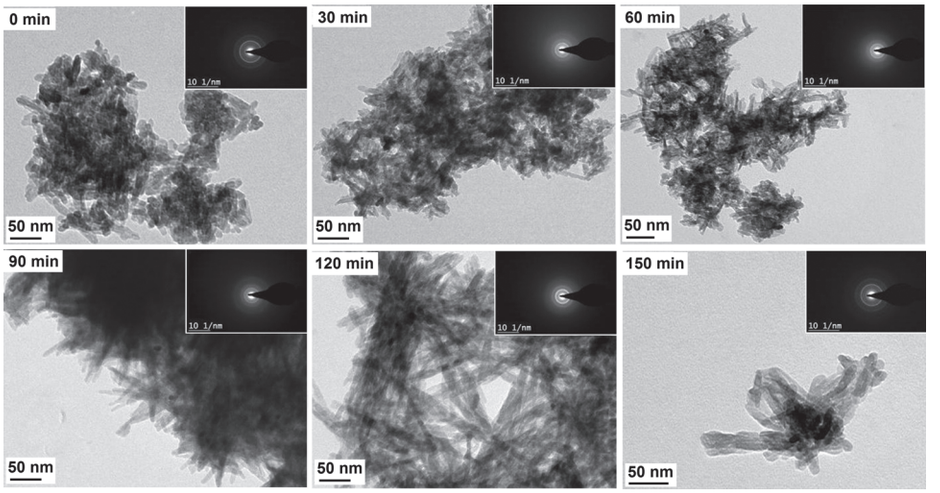

Fig. 4. TEM micrograph of synthesized CDHA with ultrasonic irradiation time. Inserts are their respective SAED pattern.

crystallite size for 60 to 120 minutes of ultrasonication in spite of rise in reaction temperature. During this period, the cavitation effect of the ultrasonic waves, disrupts the growth of the crystallites. But after 120 minutes the crystallite size increases again due to the rise in the reaction temperature. In other words, the sonication effect on the sample is subdued by the temperature rise. The synthesized nCDHA were thermally stable till 650 °C and upon heating to 700 °C, it showed peaks corresponding to β-TCP (JCPDS 9-169) confirming the formed phase to be calcium deficient apatite.[15]

The FT-IR spectra of samples exhibit clear evidence of CDHA by the presence of HPO_4^{2-} ion bands at 875 cm^{-1} shown in Figure 3.[19,20] Assignments of observed infrared frequencies (cm^{-1}) of synthesized samples are given in Table II. The FTIR of all samples showed pattern similar to CDHA synthesized by microwave irradiation.[15] The samples showed low intense OH^- bands than stoichiometric HAp supporting the loss of OH^- ions from the unit cell. The internal modes corresponding to the PO_4^{3-} groups and bands corresponding to adsorbed H_2O and CO_3^{2-} ions were also noted.[21] The HPO_4^{2-} band was not observed for samples heat treated as reported that conversion of HPO_4^{2-} to $P_2O_7^{4-}$ occurs above 200 °C.[16]

The TEM micrograph unveils the change in morphology of the particles through ultrasonication. Figure 4 clearly shows the particles without ultrasonication are seen to have non-homogeneous shapes whereas uniform rods for 90 min of ultrasonication and needle-like for 120 minutes of ultrasonication was observed. Further, TEM micrograph indicates the elongation of particle in the [0001] direction. So, it can be said that the ultrasonication has lead to increase in the aspect ratio of the particles with time of ultrasonication. Moreover, fused ring SAED pattern also confirms the nanocryatallinity of CDHA. Overall, ultrasonication on CDHA nanoparticle formation showed improved nanocrystallanity, and increased crystal aspect ratio with needle-like morphology. Therefore, sonochemical process is a simple and elegant choice of synthesizing CDHA nanoparticles.

4. CONCLUSIONS

The exposure of ultrasonic radiation during the synthesis of CDHA results in the formation of nanoparticles as characterized by XRD, FTIR, TEM and SAED techniques. The nanoparticles were confirmed to be the apatite phase with the existence of HPO_4^{2-} group characteristics of CDHA. The size, shape and fraction of crystallinity of the nanoparticles exhibits non-uniform behaviour according to sonication time. The ultrasonication of CDHA nanoparticles showed improved nanocrystallinity and the possibility of tailoring its morphology. Therefore, sonochemical process is a good choice of synthesizing CDHA nanoparticles among the other conventional methods.

References and Notes

1. P. W. Brown and B. Constantz, Hydroxyapatite and Related Materials, CRC Press, Boca Raton, USA **(1994)**.
2. (a) K. J. L. Burg, S. Porter, and J. F. Kellam, Biomaterial developments for bone tissue engineering. *Biomater.* 21, 2347 **(2000)**; (b) M. Ramalingam, M. Young, V. Thomas, L. Sun, L. Chow, C. Tison, K. Chatterjee, W. Miles, and C. Simon, Nanofiber scaffold gradients for interfacial tissue engineering. *J. Biomater. Appl.* 27, 695 **(2013)**; (c) R. Murugan and S Ramakrishna, Development of cell-responsive nanophase hydroxyapatite for tissue engineering. *Am. J. Biochem. Biotech.* 3, 118 **(2007)**.
3. K. Lewis, A. Choi, J. Chou, and B. B. Nissan, Nanoceramics in medical application. *Materials Australia* 40, 32 **(2007)**.
4. G. Bezzi, G. Celotti, E. Landi, T. M. G. La Torretta, I. Sopyan, and A. Tampieri, A novel sol–gel technique for hydroxyapatite preparation. *Mater. Chem. Phy.* 78, 816 **(2003)**.
5. H. Q. Zhang, S. P. Li, and Y. H. Yan, Dissolution behaviour of hydroxyapatite in hydrothermal solution. *Ceram. Int.* 27, 451 **(2001)**.
6. H. S. Liu, T. S. Chin, L. S. Lai, S. Y. Chiu, K. H. Chuang, C. S. Chang, and M. T. Lui, Hydroxyapatite synthesized by a simplified hydrothermal method. *Ceram. Int.* 23, 19 **(1997)**.

7. P. Luo and T. G. Nieh, Synthesis of ultrafine hydroxyapatite particles by a spray dry method. *Mater. Sci. Eng. C* 3, 75 **(1995)**.

8. A. C. Tas, Synthesis of hydroxyapatite and application in bone and dental regeneration in human body. *J. Euro. Ceram. Soc.* 20, 2389 **(2000)**.

9. B. Vaidhyanathan and K. J. Rao, Rapid microwave assisted synthesis of hydroxyapatite. *Bull. Mater. Sci.* 19, 1163 **(1996)**.

10. K. Itatani, K. Iwafune, F. S. Howell, and M. Aizawa, Preparation of various calcium-phosphate powders by ultrasonic spray freeze-drying technique. *Mater. Res. Bull.* 35, 575 **(2000)**.

11. W. Kim and F. Saito, Sonochemical synthesis of hydroxyapatite from H_3PO_4 solution with $Ca(OH)_2$. *Ultrasonics Sonochem.* 8, 85 **(2001)**.

12. D. Gopi, K. M. Govindaraju, C. A. P. Victor, L. Kavitha, and N. Rajendiran, Spectroscopic investigations of nanohydroxyapatite powders synthesized by conventional and ultrasonic coupled sol–gel routes. *Spectrochim. Acta Mol. Biomol. Spec.* 70, 1243 **(2008)**.

13. G. E. Poinern, R. K. Brundavanam, N. Mondinos, and Z. T. Jiang, Synthesis and characterisation of nanohydroxyapatite using an ultrasound assisted method. *Ultrasonics Sonochem.* 16, 469 **(2009)**.

14. S. Manafi and S. H. Badiee, Effect of ultrasonic on crystallinity of nano-hydroxyapatite via wet chemical method. *Iranian J. Pharma. Sci.* 4, 163 **(2008)**.

15. A. Siddharthan, S. K. Seshadri, and T. S. Sampath kumar, Microwave accelerated synthesis of nanosized calcium deficient hydroxyapatite. *J. Mater. Sci. Mater. Med.* 15, 1279 **(2004)**.

16. A. Siddharthan, S. K. Seshadri, and T. S. Sampath Kumar, Rapid synthesis of calcium deficient hydroxyapatite nanoparticles by microwave irradiation. *Trends Biomater. Artificial Organ* 18, 110 **(2005)**.

17. A. Mortier, J. Lemaitre, and P. G. Rouxhet, Temprature-programmed characterization of synthetic calcium-deficient phosphate apatites. *Thermochim. Acta* 143, 265 **(1989)**.

18. K. H. Prakash, C. P. Ooi, R. Kumar, K. A. Khor, and P. Cheang, Effect of super saturation level on the size and morphology of hydroxyapatite precipitate. *NanoSingapore: IEEE Conference on Emerging Technologies–Nanoelectronics*, Singapore **(2006)**, Vol. 345–349.

19. S. Koutsopoulos, Synthesis and characterization of hydroxyapatite crystals: A review study on the analytical methods. *J. Biomed. Mater. Res.* 62, 600 **(2002)**.

20. R. M. Wilson, J. C. Elliot, and S. E. P. Dowker, Formate incorporation in the structure of Ca-deficient apatite: Rietveld structure refinement. *J. Solid State Chem.* 174, 132 **(2003)**.

21. S. C. Liou, S. Y. Chen, H. Y. Lee, and J. S. Bow, Structural characterization of nano-sized calcium deficient apatite powders. *Biomater.* 25, 189 **(2004)**.

22. K. A. Bhat, R. Padmavathi, and D. Sangeetha, Chlorotrimethyl silane coupled chitosan/polyacrylamide/nano hydroxyapatite composites for controlled drug release applications. *J. Biomater Tissue Eng.* 2, 244 **(2012)**.

23. C. P. Dhanalakshmi, L. Vijayalakshmi, and V. Narayanan, *In situ* preparation and characterisation of nano carbonated hydroxyapatite/poly(4-vinyl pyridine-co-styrene) composite and its biomedical application. *J. Biomater Tissue Eng.* 2, 314 **(2012)**.

Received: 19 January 2014. Accepted: 14 February 2014.